

# Linear instability of uniform shear currents on the $\beta$ -plane

Nathan Paldor<sup>1</sup>, Yona Dvorkin<sup>2</sup> and Doron Nof<sup>3</sup>

<sup>1</sup> Fredy and Nadine Herrmann Institute of Earth Sciences, The Hebrew University of Jerusalem, Edmond J. Safra Campus, Givat Ram, Jerusalem 91904 Israel. Email: [nathan.paldor@huji.ac.il](mailto:nathan.paldor@huji.ac.il)

<sup>2</sup> Geological Survey of Israel, 30 Malchei Yisrael St., Jerusalem, 95501 Israel. Email: [yona@gsi.gov.il](mailto:yona@gsi.gov.il)

<sup>3</sup> Department of Earth, Ocean and Atmospheric Sciences, Florida State University, 117 N. Woodward Ave., Tallahassee, FL 32306 USA. Email: [nof@ocean.fsu.edu](mailto:nof@ocean.fsu.edu)

29/April/2011

*J. Mar. Res.* – In Submission

A personal note from Nathan Paldor: I was Melvin Stern's a Ph.D. student in the Graduate School of Oceanography of the University of Rhode Island between 1979 and 1982. Melvin proposed the f-plane version of the present study as the topic of my Ph.D. thesis and I am happy to extend Melvin's 30 year old idea to the  $\beta$ -plane in this tribute to my great mentor and an inspiring scientist. I will always cherish the great moments I had when we discussed various Geophysical Fluid Dynamical problems in the course of my Ph.D. studies and in subsequent years when he moved to FSU.

## **Abstract**

A unified formulation of the instability of a mean flow with uniform shear is proposed, which includes both the coupled density front and the coastal current. The unified formulation shows that the previously found instabilities of the coupled density front on the f-plane has natural extension to coastal currents, where the instability exists provided the net transport by the current is sufficiently small. This extension of the coupled front instability to coastal currents implies that the instability originates from the interaction between Inertia-Gravity waves and a vorticity edge wave and not from the interaction of the two edge waves that exist at the two free streamlines due to the Potential Vorticity jump there. The present study also extends these instabilities to the  $\beta$ -plane and is shows that  $\beta$  slightly destabilizes the currents by adding instabilities in wavelength ranges that are stable on the f-plane but has little effect on the growthrates in wavelength ranges that are unstable on the f-plane. An application of the  $\beta$ -plane instability theory to the generation of rings in the retroflection region of the Agulhas current yields a very fast perturbation growth of the scale of 1 day and this fast growthrate is consistent with the observation that at any given time, as many as 10 Agulhas rings can exist in this region.

## **1. Introduction**

The study of linear instabilities that develop as small amplitude, wavelike, perturbations on a mean current is greatly simplified by assuming that the latter is typified by a uniform lateral shear. In cases when the height (thickness) of layer of fluid under study vanishes along a contour (e.g. when the isopycnal that bounds the layer from below, shoals until it intersects the ocean's surface along a line commonly referred to as a free streamline) the mean shear has to equal the Coriolis frequency for the mean potential vorticity to be finite (i.e. non-singular).

On the  $f$ -plane the assumptions regarding the uniform shear (that equals  $f_0$ ) leads, via the geostrophic balance, to a parabolic sea-surface height in the case of a barotropic ocean (and a parabolic interface depth in the equivalent-barotropic set-up). This physical set-up described above was studied in the past in two cases (both are depicted in Fig. 1): the coupled density front, where the interface that bounds the upper layer intersects the free surface along two lines (panel (a)), and the coastal current where the mean flow is bounded on one side by a vertical wall (panel (b)).

An analytic theory of the instability of a coupled density front was proposed by Griffiths, Killworth and Stern (1982, GKS hereafter), where the theoretical estimations (made up of analytical calculations for long waves and their numerical extension to short waves) were compared with laboratory experiments. The original theory of GKS was subsequently extended in Paldor and Ghil (1990) to the 2-layer case, where the dynamics of the lower layer is coupled with that of the upper layer by the hydrostatic relation (and this coupling is due to the finite depth of the lower layer). The main new finding of Paldor and Ghil (1990) is the calculation of additional instabilities that prevail in discontinuous wavenumber bands and these instabilities exist due to the interaction of other modes than those whose interaction is responsible for the instability discovered by GKS. In addition, Paldor and Ghil (1990) have also shown that in a two-layer ocean in which the lower is sufficiently thin, a continuous shortwave instability exists in which the growthrate increases linearly with the wavenumber. Recently, Scherer and Zeitlin (2008) have demonstrated numerically that the isolated instability bands of the coupled density front originate from the coalescence of real modes: Inertia-gravity modes; standing modes (where the real part of the phase speed vanishes) and vorticity modes (associated with potential vorticity discontinuity at the free streamlines).

In the case of the uniform shear current, shown in panel (b) of Fig. 1, Paldor (1983) showed that this current is stable on the  $f$ -plane provided the flow is uni-directional and the sufficiently high (i.e. the minimal speed is above some threshold value). However, the numerical search has not detected any instability even when the current has a retrograde segment near the coast (i.e. a part of the current that flows backwards relative to the off-coast part) so its mean speed is below the threshold value. This case was extended to a two-layer set-up in Paldor and Ghil (1991), and a continuous unstable mode was found for sufficiently shortwave perturbations. However, the stability of this current was never investigated on the  $\beta$ -plane.

Despite the different boundary conditions, the two uniform shear cases are analyzed in the present study in a single theory. We use a unified formulation that applies to both to the coastal current case, where the physical boundary condition is “no normal flow” at the coast and the coupled density front, where the physical boundary condition at the right free streamline is regularity of the solutions. This unified formulation is applied to the instability study of the two cases on the  $\beta$ -plane, where both the mean flows and the perturbation equations are more cumbersome than on the  $f$ -plane.

The paper is organized as follows: The unified formulation of the instability problem of the uniform shear flow on the  $\beta$ -plane in the two cases is developed in section 2. In section 3 we deduce analytical constraints of the instability theory on the  $f$ -plane and in section 4 we calculate numerically the instabilities that follow from this unified formulation. The study ends with a discussion in section 5.

## **2. A unified formulation of the instability problem of coastal currents and coupled density fronts**

We consider the Shallow Water Equations (SWE) on the  $\beta$ -plane:

$$\begin{aligned}
\frac{\partial v}{\partial t} + u \frac{\partial v}{\partial x} + v \frac{\partial v}{\partial y} + u(f_0 + \beta y) &= -g \frac{\partial h}{\partial y}, \\
\frac{\partial u}{\partial t} + u \frac{\partial u}{\partial x} + v \frac{\partial u}{\partial y} - v(f_0 + \beta y) &= -g \frac{\partial h}{\partial x}, \\
\frac{\partial h}{\partial t} + \frac{\partial(hu)}{\partial x} + \frac{\partial(hv)}{\partial y} &= 0.
\end{aligned} \tag{1}$$

where,  $(x, y)$  are the Cartesian coordinates in the (East, North) directions,  $t$  is time,  $(u, v)$  are the component of the velocity vector in the  $(x, y)$  directions,  $h$  is the depth (thickness) of the layer, and  $g$  is the reduced gravity. The Coriolis frequency,  $f$ , is assumed to vary linearly with  $y$  i.e.,  $f=f_0+\beta y$ , with  $f_0 = 2\Omega\sin(\phi_0)$  and  $\beta= 2\Omega\cos(\phi_0)/R$  (where  $\phi_0$  is the central latitude of the domain and  $R$  and  $\Omega$  are Earth's radius and frequency of rotation, respectively).

As is evident from the two panels of Fig. 1, both the coupled density front and the coastal current have the same cross-stream width,  $L$ . This mean width is used for scaling the horizontal lengths  $(x, y)$  and, when  $f_0$  is used to scale time, the natural choice for the velocity scale is  $f_0L$ . Selecting  $(f_0L)^2/g$  to be the height scale completes the scaling that is required for transforming the dimensional system (1) into its non-dimensional counterpart:

$$\begin{aligned}
\frac{\partial u}{\partial t} + u \frac{\partial u}{\partial x} + v \frac{\partial u}{\partial y} - v(1 + \varepsilon y) &= -\frac{\partial h}{\partial x}, \\
\frac{\partial v}{\partial t} + u \frac{\partial v}{\partial x} + v \frac{\partial v}{\partial y} + u(1 + \varepsilon y) &= -\frac{\partial h}{\partial y}, \\
\frac{\partial h}{\partial t} + h \frac{\partial v}{\partial x} + v \frac{\partial h}{\partial y} + h \frac{\partial u}{\partial x} + u \frac{\partial h}{\partial x} &= 0,
\end{aligned} \tag{2}$$

where  $\varepsilon = \frac{\beta L}{f_0} = \cot(\phi_0) \frac{L}{R}$ . For  $L \approx 400$  km and  $\cot(\phi_0) \approx 1.6$  (near  $35^\circ$  latitude) the small

parameter  $\varepsilon$  is about 0.1. At higher latitudes (poleward of  $35^\circ$ ) and for narrower (less than 400 km) currents the value of  $\varepsilon$  is smaller than 0.1.

We now assume that a basic (mean) state exists, and that it is made up of  $\bar{u}(y)$ ,  $\bar{h}(y)$  that are in geostrophic balance with no  $x$  or  $t$  dependence. The small amplitude perturbations (linear) about this basic state are the focus of the search for instabilities. Since geostrophy provides only one relationship between  $\bar{u}(y)$  and  $\frac{\partial \bar{h}(y)}{\partial y}$ , another constraint is needed to uniquely determine both  $\bar{u}(y)$  and  $\bar{h}(y)$ . Such an assumption is the uniformity of the mean shear. The uniform value of this shear has to be set equal to the mean Coriolis frequency (i.e. the absolute vorticity vanishes identically) in order to guarantee that the potential vorticity is non-singular even at the free streamline(s).

The dimensional assumption on the (regular) uniformity of the mean flow,  $\frac{\partial u}{\partial y} = f_0$ , takes

the non-dimensional form:  $\frac{\partial \bar{u}}{\partial y} = 1$  and when this is added to the (non-dimensional)

geostrophic balance on the  $\beta$ -plane,  $\bar{u} = -\frac{1}{1+\varepsilon y} \frac{\partial \bar{h}}{\partial y}$ , one obtains:

$$\begin{aligned}\bar{u}(y) &= y + U_0 \\ \bar{h}(y) &= -\frac{\varepsilon y^3}{3} - \frac{y^2}{2}(1 + \varepsilon U_0) - U_0 y = -\frac{y^2}{2} - U_0 y - \varepsilon \left( \frac{y^3}{3} + U_0 \frac{y^2}{2} \right)\end{aligned}$$

where  $U_0$  is the mean velocity at  $y=0$  (the left free streamline). From the last expression for

the mean thickness it is clear that  $\bar{h}(-1) = U_0 - \frac{1}{2} + \varepsilon \left( \frac{1}{3} - \frac{U_0}{2} \right)$  so for  $\bar{h}(-1)$  to be non-

negative,  $U_0$  has to satisfy  $U_0 \geq \frac{1-2\varepsilon}{2-\varepsilon}$ . For  $U_0 = \frac{1-2\varepsilon}{2-\varepsilon} = \frac{3-2\varepsilon}{6-3\varepsilon} \approx \frac{1}{2} \left( 1 - \frac{1}{6} \varepsilon \right)$  (and in

particular  $U_0=0.5$  for  $\varepsilon=0$ ) the mean height vanishes at the right boundary,  $y=-1$  (in addition to the left boundary,  $y=0$ ) and the coupled density front is recovered.

Having determined the basic state we now turn our attention to the perturbations. Since there are no coefficients in the SWE that depend explicitly on  $x$  or  $t$  (only  $f$  depends on  $y$ ) one can safely let the perturbations take the form of zonally propagating waves with  $y$ -dependent amplitudes:  $(u, V, h) \sim (u(y), V(y), h(y))e^{ik(x-ct)}$ .

Substituting this form into the equations for the small amplitude perturbation yields:

$$uc = \bar{u}\bar{u} - \frac{\varepsilon y V}{k^2} + h$$

$$Vc = \bar{u}V - (1 + \varepsilon y)u - \frac{\partial h}{\partial y}$$

$$hc = \frac{\bar{h}}{k^2} \frac{\partial V}{\partial y} - \frac{V}{k^2} \bar{u}(1 + \varepsilon y) + \bar{u}h + \bar{h}u,$$

where  $V = -ikv \Leftrightarrow v = V \frac{i}{k}$ . These equations can be written as a matrix-like eigenvalue

system where the phase speed,  $c$ , is the eigenvalue and  $(u(y), V(y), h(y))$  is the eigenvector:

$$\begin{pmatrix} \bar{u} & -\frac{\varepsilon y}{k^2} & 1 \\ -(1 + \varepsilon y) & \bar{u} & -\frac{\partial}{\partial y} \\ \bar{h} & -\frac{\bar{u}(1 + \varepsilon y)}{k^2} + \frac{\bar{h}}{k^2} \frac{\partial}{\partial y} & \bar{u} \end{pmatrix} \begin{pmatrix} u \\ V \\ h \end{pmatrix} = c \begin{pmatrix} u \\ V \\ h \end{pmatrix} \quad (3)$$

(the differential operator,  $\partial/\partial y$ , that appears in some of the elements of the matrix is the reason why this is not a genuine matrix eigenvalue problem).

Since the first of these equations (the upper row of the matrix) does not contain the differential operator, this algebraic relationship actually expresses  $u$  as a linear combination of  $h$  and  $V$ :

$$u = -\frac{h}{(\bar{u} - c)} + \frac{\varepsilon y V}{k^2(\bar{u} - c)}.$$

This simple expression can be employed to eliminate  $u$  from the other two equations, which yields the pair of coupled differential equations:

$$\begin{aligned}\frac{dh}{dy} &= V[\bar{u} - c - \frac{\varepsilon y}{k^2(\bar{u} - c)} - \frac{\varepsilon^2 y^2}{k^2(\bar{u} - c)}] + h[\frac{1}{(\bar{u} - c)} + \frac{\varepsilon y}{(\bar{u} - c)}], \\ \frac{\partial V}{\partial y} &= V[\frac{\bar{u}}{h}(1 + \varepsilon y) - \frac{\varepsilon y}{(\bar{u} - c)}] + h[-\frac{k^2}{h}(\bar{u} - c) + \frac{k^2}{(\bar{u} - c)}].\end{aligned}\quad (4)$$

The last step in the formulation of the problem is the transformation of this  $(h, V)$  system to a new  $(h, \psi)$  system where the variable  $\psi$  is defined by:  $\psi = V \cdot \bar{h}$ . The resulting new system is:

$$\begin{aligned}\frac{\partial h}{\partial y} &= \frac{\psi}{h}[\bar{u} - c - \frac{\varepsilon y}{k^2(\bar{u} - c)} - \frac{\varepsilon^2 y^2}{k^2(\bar{u} - c)}] + h[\frac{1 + \varepsilon y}{(\bar{u} - c)}], \\ \frac{\partial \psi}{\partial y} &= \psi[-\frac{\varepsilon y}{(\bar{u} - c)}] + h[-k^2(\bar{u} - c) + \frac{\bar{h}k^2}{(\bar{u} - c)}].\end{aligned}\quad (5)$$

The main advantage of the transformation from  $V$  to  $\psi$  is that the boundary conditions associated with system (5) are  $\psi(0) = 0 = \psi(-1)$  for both the coupled density front and the coastal current while in the  $(h, V)$  system the BC at the right boundary is  $V(-1)=0$  in the case of the coastal current while in the case of the coupled density front the condition is  $V(-1)<\infty$ . The  $(h, \psi)$  system lets one analyze the instability of the coupled density front as a particular case of the coastal current's instability where  $U_0 = \frac{3-2\varepsilon}{6-3\varepsilon}$  without changing the boundary condition at  $y=-1$ .

### 3. Stability of coastal current on the f-plane

Setting  $\varepsilon=0$  and requiring  $U_0 > 0.5$  (i.e. focusing on the coastal current) one can derive integral constraints on complex solutions of the second order differential eigenvalue system (4) for  $c=c_r+ic_i$  with  $c_i \neq 0$  (see equations 18 and 19 in Paldor, 1983). These integral constraints lead to the condition:

$$\int_0^1 |\phi|^2 (3z^2 - 2U_0z - 2|\gamma|^2) dz > 0, \quad (6)$$

where:  $z=y$  (i.e.  $z$  varies between 0 and 1),  $\gamma=U_0-c=U_0-c_r-ic_i$  and  $\phi(z(y))=u(y)$ . This integral was used in Paldor (1983) to derive the necessary condition for instability:  $U_0 < 3/2$  based on the realization that for  $U_0 > 3/2$  the integrand on the Left Hand Side of (6) is negative throughout the entire  $0 \leq z \leq 1$  domain even for vanishingly small  $\gamma$  so the integral inequality cannot be satisfied.

The unified formulation developed in the preceding section provides a natural connection between the instability of the coupled front (where  $U_0 = 0.5$ ) and the coastal current (where  $U_0 > 0.5$ ). By viewing the former problem as a particular case of the latter with  $U_0 = 0.5$  it is not clear whether the coastal current is stable throughout the  $0.5 < U_0 < 1.5$  range and the  $U_0 > 1.5$  is an over estimate of the necessary condition for instability or there is a sub-range near  $U_0 = 0.5$  where it is unstable. This f-plane issue is addressed in relation to the total transport of the current, which is also determined by  $U_0$  as follows: For  $\bar{h}(-1) = U_0 - 0.5$  and  $\bar{h}(0) = 0$  an application of the geostrophic balance to the downstream transport yields:

$$\int_{-1}^0 \bar{h} \cdot \bar{u} dy = - \int_{-1}^0 \bar{h} \cdot \bar{h}_y dy = \frac{1}{2} (\bar{h}(-1)^2 - \bar{h}(0)^2) = (U_0 - 0.5)^2 / 2.$$

At  $U_0 = 1/2$  (i.e. the coupled density front) instabilities exist and the total transport vanishes. Whether or not these instabilities prevail at  $1/2 < U_0 < 1.5$  is unclear from the available literature on the subject and this point is the first point addressed in the next section.

#### 4. Results

The numerical results shown below were calculated using two methods of solutions. The first method applied the Chebyshev collocation method (see a general description of the method in

Treffethen, 2000 and a particular recent application in De-Leon and Paldor, 2011) to system (3). For the most part, the collocation method was used to solve system (3) with 120 points (a total of 121 points, including the two boundaries) and occasionally verified the accuracy of our results by computing the eigenvalues (i.e. phase speeds) and eigenfunctions (ordered as  $u$ ,  $V$ , and  $h$ ) with 360 points. The second method is a shooting method where system (5) was integrated numerically from  $y=0$  starting with the initial conditions  $\psi(0) = 0$  and  $h(0) = 1$  (the latter is a mere trivial normalization value) to  $y = -1$  and the value of  $c$  was varied to find those values at which the boundary condition  $\psi(-1) = 0$  is satisfied (see similar application of the shooting method in Paldor and Nof, 1992; Paldor and Dvorkin, 2006). The differences between numerical results obtained with these two methods were insignificant (lying closer to one another than the widths of the curves shown in the figures below).

The instability curves (growthrates) shown in Fig. 2 are an application of the unified instability theory developed in section 2 to the coupled density front and the coastal current, on the  $f$ -plane. Setting  $\varepsilon=0$  in system (5) and letting the value of  $U_0$  increase from 0.5 (the coupled density front; upper panel) to larger values of  $U_0 = 0.56$  and  $U_0 = 0.62$  (both describe the coupled front, middle and lower panels) we notice that the instability of the coupled density front (the longwave GKS instability, as well as the additional shortwave branches) in which the boundary condition on  $V$  is its regularity at  $y = -1$ , has a natural extension to the coastal current regime despite the change of boundary condition to  $V = 0$  at  $y = -1$ . As the value of  $U_0$  increases from 0.5, the various instability branches shift to the right (shorter waves) and become smaller. As explained above,  $U_0$  determines the total transport of the mean current and the results shown in Fig. 2 demonstrate that the coastal current is stable from  $U_0 \approx 0.65$ , at which value its total transport is:  $(U_0 - 0.5)^2 / 2 \approx 0.01$ .

The effect of  $\beta$  (proportional to  $\varepsilon$ ) on the instability of the coupled density front is demonstrated in Fig. 3 by calculating the instabilities for  $\varepsilon = 0.05$  and  $\varepsilon = 0.1$  and setting  $U_0(\varepsilon)$  to the appropriate values of the coupled density front:  $U_0 = \frac{3-2\varepsilon}{6-3\varepsilon}$ . Clearly, on the  $\beta$ -plane, the instability curves widen at each of the branches and wavelength ranges that are stable on the  $f$ -plane (i.e., the ranges between the isolated branches shown in the upper panel of Fig. 2) are destabilized by  $\beta$ . On the other hand, a comparison between the maximal growth rates of the various branches in Fig. 3 and those in the upper panel of Fig. 2 shows that these maximal growth rates are hardly affected by  $\beta$ .

The  $\beta$  effect is different on the coastal current. As is evident from the results shown in Fig. 4, at  $U_0 = 0.75$  (where the coastal current was stable on the  $f$ -plane i.e.  $\varepsilon=0$ ) the shortwave instability branch near  $k = 8.4$  becomes dominant and the separate modes at longer wavelength (see Figs. 2 and 3) merged into a single continuous, slightly unstable, mode. The instability curves at  $\varepsilon = 0.05$  (not shown) are very similar to those at  $\varepsilon = 0.1$ .

The (complex) eigenfunctions associated with the unstable modes whose phase speeds were shown above have no particularly interesting structure. However, the calculation of the eigenfunction verifies our results regarding the eigenvalues since the former are calculated independently by integrating system (5) numerically using the values of  $c$  found previously at the noted values of  $\varepsilon$ ,  $U_0$  and  $k$ . An example of the eigenfunction structure is shown in Fig. 5 for the instability near  $k=8.4$  in Fig. 4 and it shows that our numerical solution for  $\psi(y)$  satisfy the boundary conditions at  $y=-1$  and  $y=0$  and that both  $h(y)$  and  $\psi(y)$  that solve system (5) are differentiable throughout the  $(-1, 0)$  interval.

## 5. Discussion

The unified formulation proposed here applies to the instability problems of the coupled density front and the coastal current on the  $f$ -plane when the shear in both mean flows is uniform. This unified formulation enables one to find the instability of the latter and when the total transport is sufficiently small and to make the connection between the two problems despite the different boundary conditions on the normal velocity in the two cases.

The effect that the variation in  $f$  (i.e., the  $\beta$  effect) has on the instability curves is quite different in the two problems: In the coupled density front,  $\beta$  shifts all the branches towards short waves and decreases their growth rates. In the coastal current a singular mode that is nearly unaffected by  $\beta$  exists at  $k = 8.4$  and a wide range instability with small growth rate exists between  $k = 0$  and  $k = 7$ . This behavior is similar to the effect of the lower layer on the coastal current (see Paldor and Ghil, 1991).

As was shown in previous studies (e.g. Scherer and Zeitlin, 2008; Paldor and Ghil, 1991) the various instability branches originate from the coalescence of different pairs of real modes in certain wavelength bands, including the particular case when the real part of the phase speed vanishes (e.g. GKS instability) which is interpreted as a standing mode. In the context of the coupled density front two waves are candidates for this coalescence: Inertia-Gravity (Poincare) waves and vorticity edge (Rossby) waves associated with the PV jump at  $y = -1$  and  $y = 0$ . Our unified formulation and the extension of these instabilities into the  $U_0 > 0.5$  region (where only one free streamline exists), imply that in the case of the coupled front ( $U_0 = 0.5$ ) the instabilities result from the interaction Inertia-Gravity waves with an edge wave and not by the interaction of the two edge waves (one at  $y = -1$  and the other at  $y = 0$ ).

The instability theory developed above can be applied to the Agulhas current near its retroflection point at  $35^\circ\text{S}$ - $40^\circ\text{S}$  latitude (see figure 6.5 in Lutjeharms, 2006). As is evident from the  $\sigma_t = 25.8$  surface, at this segment the Current has zero net transport and two free

streamlines, mimicked by the idealized cartoon shown in panel (a) of Fig. 1 – the coupled density front. For the relevant oceanographic parameters:  $L = 300$  km (Current's mean width at the retroflection region);  $\phi_0=0.65$  (south latitude of  $37.5^\circ$ ) one obtains  $\varepsilon=0.06$  (so  $U_0$  is about 0.492) and the two lower panels of Fig. 3 show that at this  $\varepsilon$  the current is unstable at all wavelengths. The maximum growthrate in both  $\varepsilon = 0.05$  and  $\varepsilon = 0.1$  panels occurs at  $k = 2.2$  so half the wavelength of the most unstable wave is  $(\pi/2.2)*300$  km  $\approx 450$  km and the growthrate at  $k = 2.2$  (for both values of  $\varepsilon$ ) is 0.15 so the time scale for the growth of the most unstable mode is:  $1/(0.15*f_0) \sim 1$  day. The 450 km estimate of the size of the Agulhas eddies based on half the wavelength of the most unstable mode is consistent with observations of the diameter of rings shed off from the Current at the retroflection region (see the discussion on P. 170 in Lutjeharms, 2006). The very fast perturbation growth (about 1 day) is consistent with the observation that more than 10 rings may exist at any given time in the Cape basin just south-west of Cape Town (see figure 6.19 and the discussion on P. 173 of Lutjeharms, 2006).

### **Acknowledgement**

Financial support for this study was provided by the US-Israel Bi-national Science Foundation (BSF) via grant number 2006296 to HU and FSU. Initial calculations of the instability curves shown in section 4 were done by A. Lokshin and D. Begun of HU. We also thank Y. Cohen of HU for his help in the production of figure 1.

## References

- De-Leon, Y. and N. Paldor. 2011. Zonally propagating wave solutions of Laplace Tidal Equations in a baroclinic ocean of an aqua-planet. *Tellus*, 63A, 348-353.
- Griffiths, R. W., P. D. Killworth and M. E. Stern. 1982. Ageostrophic instability of ocean currents. *J. Fluid Mech.*, 117, 343-377.
- Lutjeharms, J. R. E. 2006. *The Agulhas Current*. Springer, 329 pp.
- Paldor, N. 1983. Stability and stable modes of coastal fronts. *Geophys. Astrophys. Fluid Dyn.*, 27, 217–228.
- Paldor, N. and Y. Dvorkin. 2006. Barotropic instability of a zonal jet: From nondivergent perturbations on the  $\beta$ -plane to divergent perturbation on a sphere. *J. Phys. Oceanogr.*, 36(12), 2271-2281.
- Paldor, N. and M. Ghil. 1990. Finite wavelength instabilities of a coupled density front. *J. Phys. Oceanogr.*, 20(1), 114–123.
- Paldor, N. and M. Ghil. 1991. Shortwave instabilities of coastal currents. *Geophys. Astrophys. Fluid Dyn.*, 58, 225–242.
- Paldor, N. and D. Nof. 1990. Linear instability of an anticyclonic vortex in a two-layer ocean. *J. Geophys. Res.*, 95(C10), 18,075 – 18,079.
- Scherer, E. and V. Zeitlin. 2008. The instability of coupled geostrophic density fronts and its nonlinear evolution. *J. Fluid Mech.*, 613, 309-327.

## Figures and Captions

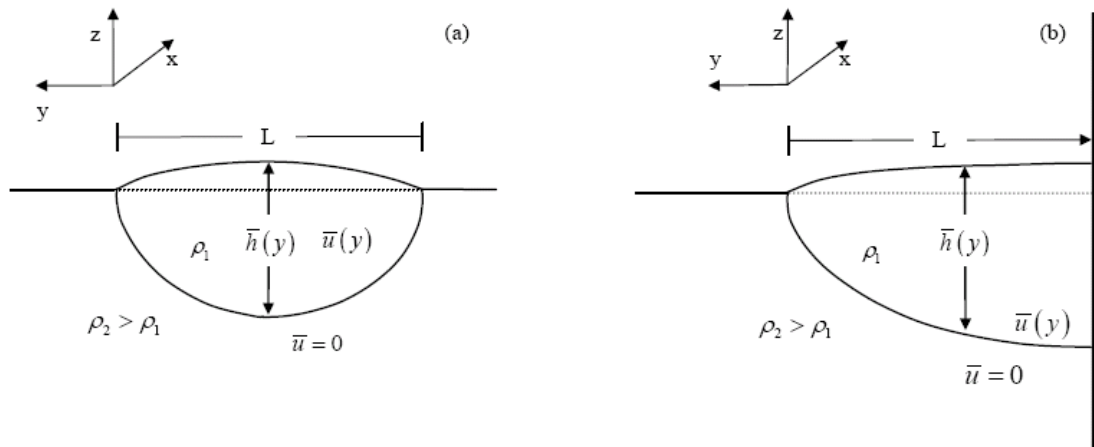


Figure 1: The coupled density front (a, left) and the coastal current (b, right) with uniform mean shear. On the  $f$ -plane, geostrophy yields a parabolic interface cross-stream variation. In the coastal current, the flow is uni-directional when the interface slopes monotonically throughout the entire domain whereas a return flow exists near the coast when the slope changes sign (which occurs on the  $f$ -plane when  $U_0 < 1$ ).

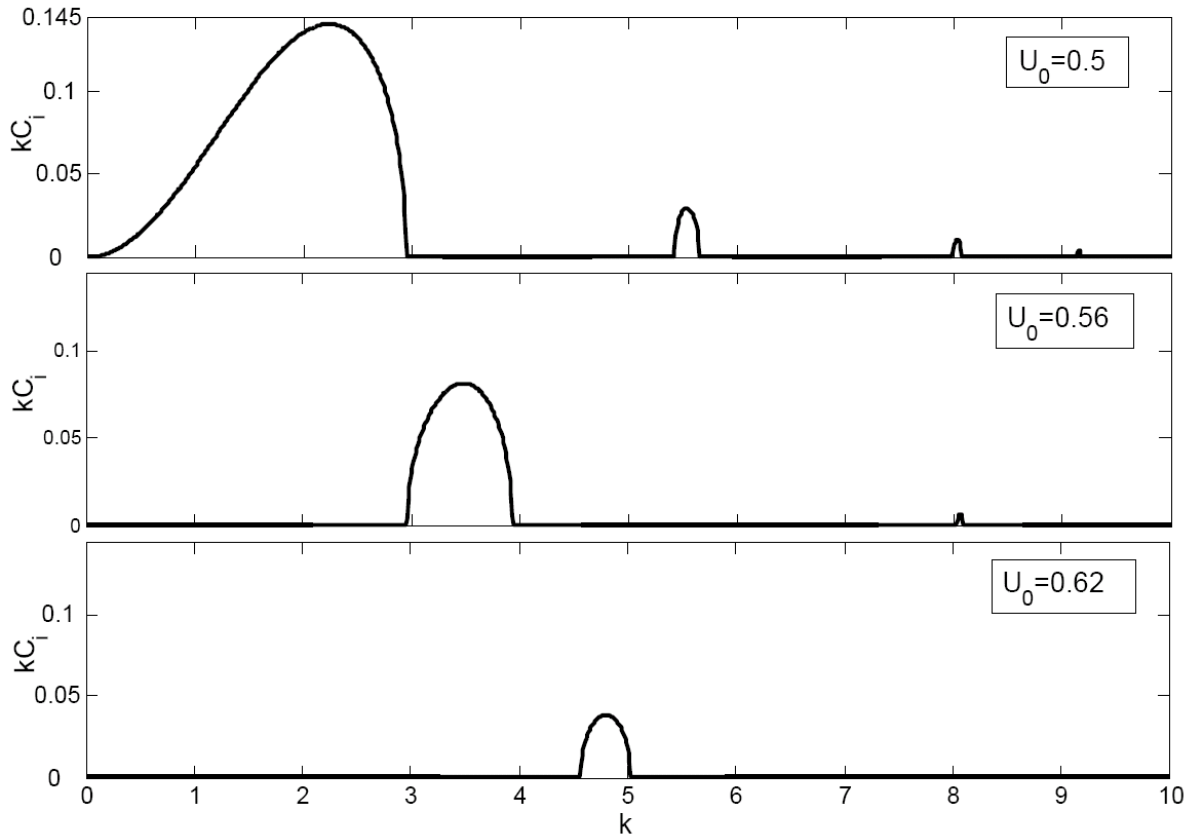


Figure 2: Instability curves,  $kC_i(k)$ , of the coupled density front ( $U_0=1/2$ , upper panel) and the coastal current ( $U_0>1/2$ , middle and lower panels) on the f-plane ( $\varepsilon=0$ ). The similarity between the two instabilities is evident despite the different V-boundary condition (but not that of  $\psi$ ) employed in the two problems. These instabilities vanish for  $U_0 \geq 0.65$ .

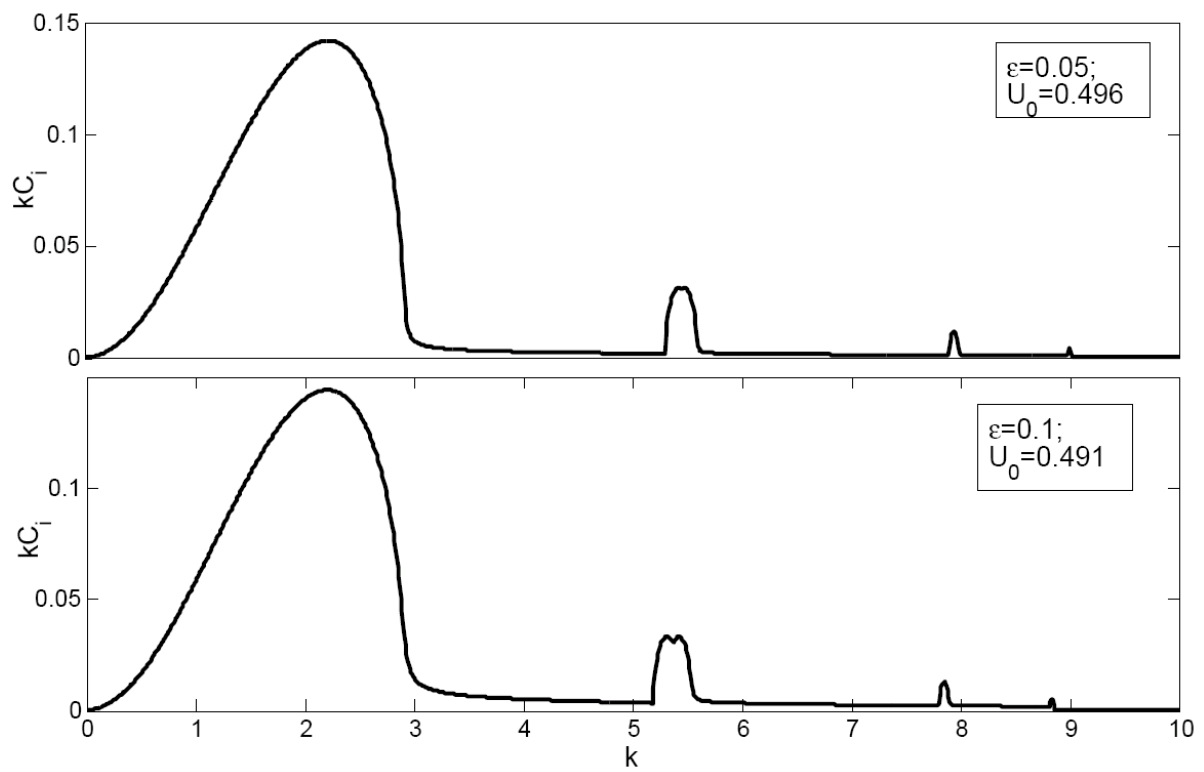


Figure 3: The  $\beta$ -effect (i.e.  $\varepsilon \neq 0$ ) on the instability of the coupled density front (i.e. when  $U_0 = (3-2\varepsilon)/(6-3\varepsilon)$ ). Clearly, a comparison of these plots with the upper panel of Figure 2 shows that  $\beta$  destabilizes the front in wavelength ranges that are stable on the f-plane but hardly affects the ranges that are unstable on the f-plane.

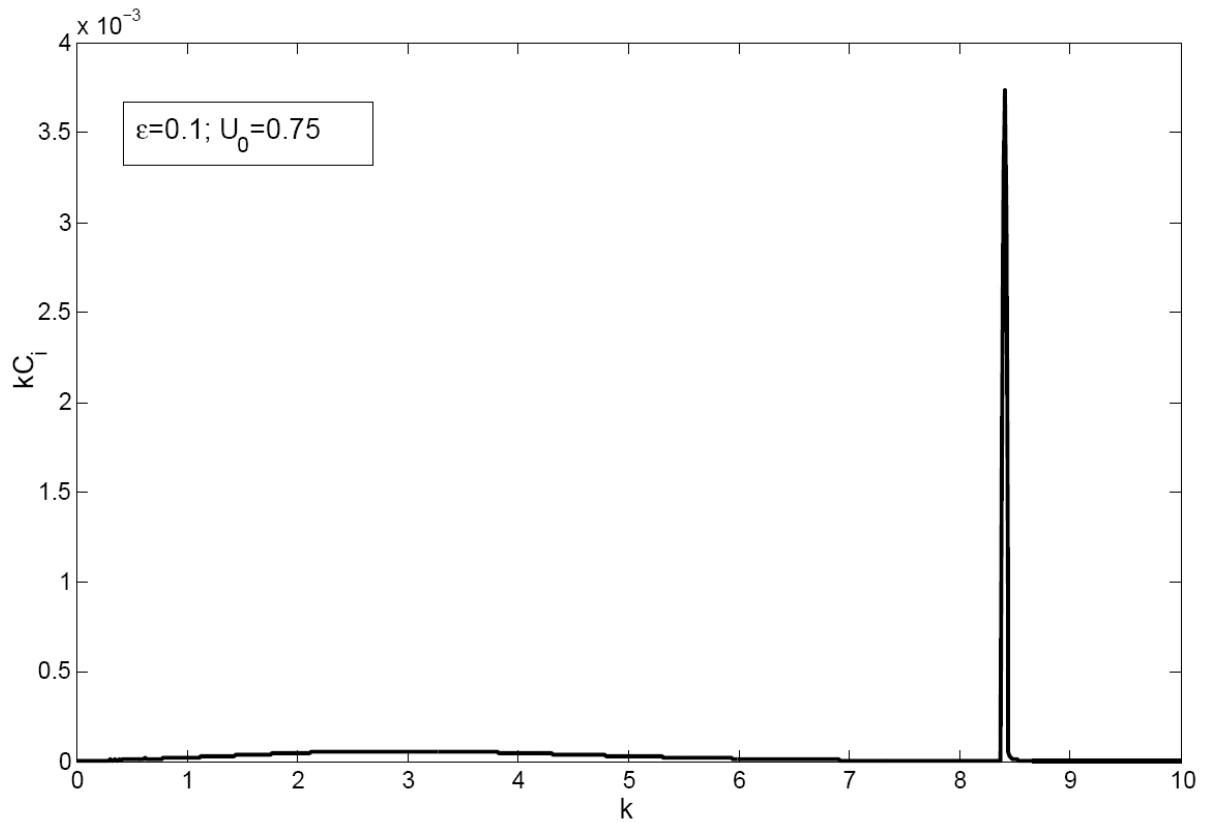


Figure 4: The effect of  $\beta$  (i.e.  $\varepsilon$ ) on the instability of the coastal current at  $\varepsilon=0.1$  and  $U_0=0.75$ , (i.e. above the threshold value of 0.65 above which no instabilities exist on the f-plane). A large range of wavelength becomes slightly unstable and at the narrow range near  $k=8.4$  a dominant but narrow branch arises where the maximal growthrate is about 0.0035, much larger than at lower values of  $k$ . The narrow branch with sharp peak near  $k=8.4$  is similar in width and magnitude to the shortwave branches near  $k=8$  and  $k=9$  in Figure 3

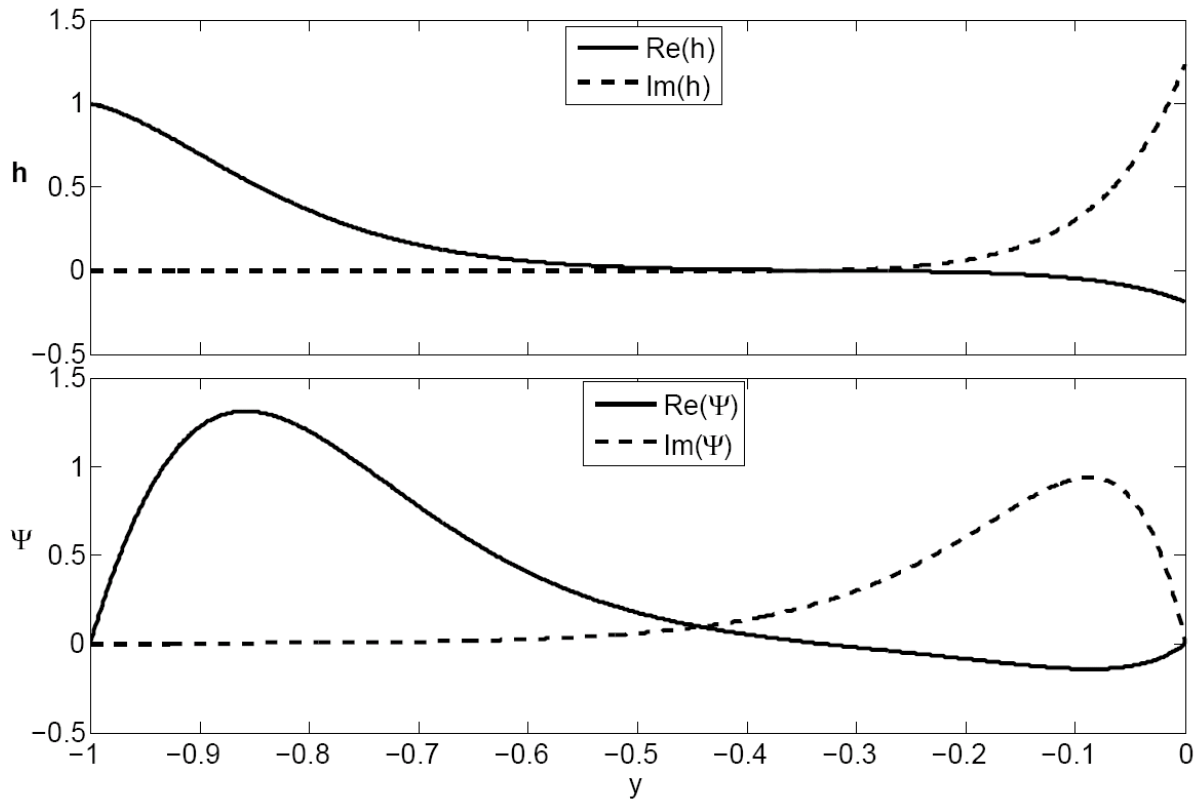


Figure 5. The  $(h(y), \psi(y))$  eigenfunctions for  $\varepsilon=0.1$  and  $U_0=0.75$  at  $k=8.4$  (the "spike" in Figure 4). The complex phase speed is:  $c=0.414+0.44 \cdot 10^{-3}$  and despite the singularity at  $y=-0.336$  of the (real part of the) coefficients  $(\bar{u}(y)-c)^{-1} = (U_0 + y - c)^{-1}$  that appear in system (5), the complex eigenfunctions are smooth everywhere, including at  $y=-0.336$ .